

# Surface Acoustic Wave Propagation Properties in AlN/3C–SiC/Si Composite Structure

Chih-Ming Lin<sup>1</sup>, Yung-Yu Chen<sup>2</sup>, Valery V. Felmetzger<sup>3</sup>, Ting-Ta Yen<sup>1</sup>, Wei-Cheng Lien<sup>1</sup>,  
Debbie G. Senesky<sup>1</sup>, and Albert P. Pisano<sup>1</sup>

<sup>1</sup>Berkeley Sensor and Actuator Center  
University of California at Berkeley  
Berkeley, California 94720, USA

<sup>2</sup>Department of Mechanical Engineering  
Tatung University  
Taipei 10452, Taiwan

<sup>3</sup>PVD Product Group  
OEM Group Incorporated  
Gilbert, Arizona 85233, USA

**Abstract**—Highly *c*-axis oriented aluminum nitride (AlN) films were grown on epitaxial cubic silicon carbide (3C–SiC) layers on Si (100) substrates using alternating current (AC) reactive magnetron sputtering at temperatures between 300 °C to 450 °C. The AlN thin films were characterized by X-ray diffraction, scanning electron microscope, and transmission electron microscopy. Two-port surface acoustic wave (SAW) devices were fabricated on the AlN/3C–SiC/Si layered structure. The SAW propagation properties in the AlN/3C–SiC/Si layered structure were theoretically and experimentally investigated. The Rayleigh mode exhibited a high acoustic velocity of 5,200 m/s due to the epitaxial 3C–SiC layer. The results demonstrate the potential of AlN thin films grown on epitaxial 3C–SiC layers to create piezoelectric acoustic devices for frequency control and harsh environment applications.

**Keywords**—Surface Acoustic Wave Devices, Aluminum Nitride, Epitaxial Cubic Silicon Carbide, Harsh Environment, Green's Function.

## I. INTRODUCTION

Diamond has the highest acoustic wave velocity among all materials because of the high Young's modulus (1035 GPa). Therefore, the zinc oxide (ZnO) thin film grown on the polycrystalline diamond layer is a good candidate for high-frequency surface acoustic wave (SAW) devices [1]–[3]. However, the polycrystalline diamond starts to decompose in strong oxidation environments upon 600 °C [4], making SAW devices on ZnO/diamond layered structures not preferred for harsh environment applications.

In contrast to diamond, silicon carbide (SiC) is another excellent candidate of the substrate for high-frequency layered SAW devices because SiC has the Young's modulus as high as 700 GPa [5] and low-loss SAW propagation properties [6]. Therefore, layered SAW devices on ZnO/6H–SiC substrates [6] and ZnO/3C–SiC/Si substrates [7] have been studied, respectively. In addition, SiC is stable to the sublimation temperature which is above 2000 °C, and exhibits the good chemical resistance to acids as well as bases, making SiC an excellent material for high-frequency and harsh environment applications [5].

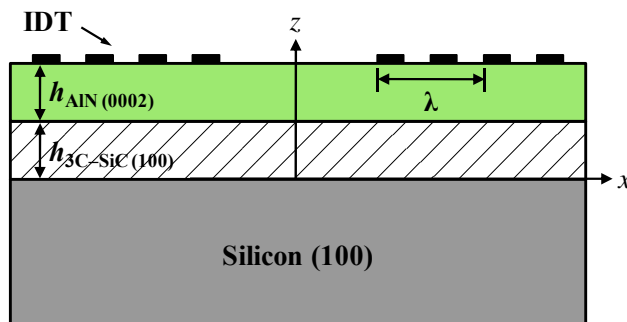


Figure 1. Illustration of the cross-section of the layered surface acoustic wave (SAW) device on the AlN/3C–SiC/Si composite structure.

As is well known, aluminum nitride (AlN) is widely applied to radio frequency (RF) acoustic devices because of its relatively high piezoelectric coefficient, CMOS compatibility, and high acoustic velocity of 12,000 m/s. Furthermore, AlN and hexagonal SiC exhibit the well-matched thermal expansion coefficient and low lattice mismatch [8]. AlN can maintain its piezoelectric properties at high temperatures as well [9]–[11]. Therefore, several research efforts have been made in this respect to establish processes to construct SAW devices using AlN/4H–SiC [12] or AlN/6H–SiC [13] layered structure. However, the manufacturing cost of the single crystal hexagonal SiC wafers obstructs the development of SiC used for the substrates of high-frequency SAW device.

In fact, for layered SAW devices, the thickness of the high velocity substrate usually needs within 20–50  $\mu\text{m}$ , depending on the operating frequency of SAW devices so the use of the single crystal hexagonal SiC wafer is extravagant. To date, the growth of epitaxial 3C–SiC films on silicon (Si) substrates have been demonstrated [5]. The use of the Si substrate is advantageous because Si is low-cost and various Si bulk micromachining techniques are well-established.

In this study, highly *c*-axis oriented AlN thin films grown on epitaxial 3C–SiC layers on Si (100) substrates using AC reactive magnetron sputtering are characterized. Although AlN (0002) and 3C–SiC (100) have a lattice mismatch of

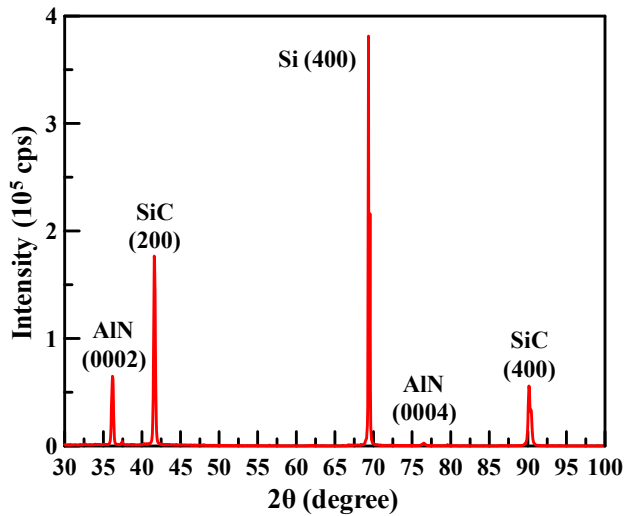


Figure 2. XRD spectrum of the AlN/3C-SiC/Si layered structure where AlN is 1  $\mu\text{m}$  and 3C-SiC is 2.3  $\mu\text{m}$ .

28.6%, this challenge was addressed by a two-step deposition process [14]. Fig. 1 illustrates SAW devices on the AlN/3C-SiC/Si layered structure. The SAW propagation properties in the AlN/3C-SiC/Si composite structure were theoretically investigated using the effective permittivity and Green's function method [3]. The expected Rayleigh mode exhibits a high acoustic velocity of 5,200 m/s which shows the potential of AlN thin films grown on epitaxial 3C-SiC layers to create high-frequency SAW devices for frequency control and harsh environment applications.

## II. GROWTH OF ALN (0002) THIN FILMS ON EPITAXIAL 3C-SiC LAYERS ON Si (100) SUBSTRATES

In this study, 2.3- $\mu\text{m}$ -thick epitaxial 3C-SiC layers grown on Si (100) wafers which were purchased from the NOVASiC Inc. were used as the substrates. AlN films were deposited on epitaxial 3C-SiC layers by AC (40 kHz) powered S-Gun magnetron [15]. Prior to AlN film deposition, the surface of the epitaxial 3C-SiC layer was treated by low energy (150–200 eV) Ar ions from capacitively coupled RF (13.56 MHz) plasma. To mitigate the effect of the lattice mismatch between AlN (0002) and 3C-SiC (100), a 50-nm-thick AlN seed layer was deposited with high nitrogen ( $\text{N}_2$ ) concentration in argon (Ar) and  $\text{N}_2$  gas mixture [14]. These initial grains served as the seeds for the growth of higher quality columnar grains as the AlN film thickness increased.

The deposition processes were performed at the ambient temperature (300–350  $^\circ\text{C}$ ) in the sputtering chamber for the majority of the AlN film thickness but at an elevated temperature (nearly 450  $^\circ\text{C}$ ), using an external infrared heater, for the 50-nm-thick AlN seed layer. The S-Gun magnetron was powered with an AC power of 3 kW during the seed layer deposition and 5.5 kW during the deposition of the remaining AlN film, providing a deposition rate of 66 nm/min. The crystalline structure was determined by X-ray diffraction (XRD, Siemens D5000) as shown in Fig. 2 where the diffraction peaks correspond to a hexagonal wurtzite-type AlN (0002) film, a cubic zinc-blende-type SiC (100) film, and a Si (100) substrate, respectively. The presence of (0002) and

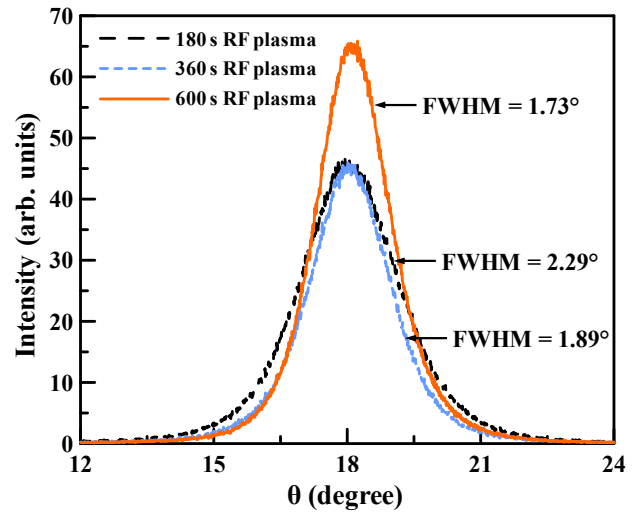


Figure 3. Rocking curve of 1- $\mu\text{m}$ -thick AlN (0002) films deposited on the epitaxial 3C-SiC (100) layer with different RF plasma etching duration.

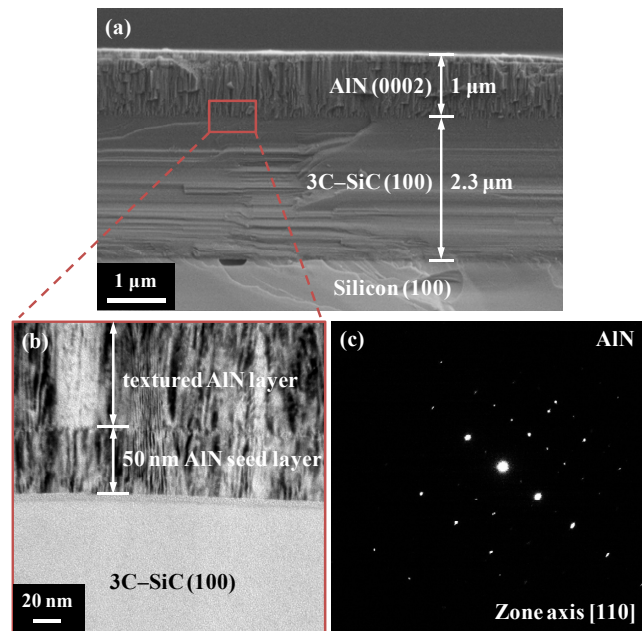


Figure 4. (a) Cross-sectional SEM image of 1- $\mu\text{m}$ -thick AlN (0002) film on the epitaxial 3C-SiC layer on the Si (100) substrate. (b) Cross-sectional BF TEM image of the interface between AlN and 3C-SiC layers. (c) Electron diffraction (ED) patterns of 1- $\mu\text{m}$ -thick AlN (0002) film grown on the epitaxial 3C-SiC (100) layer along the [110] zone axis.

(0004) AlN reflections at  $36.07^\circ$  and  $76.46^\circ$ , respectively give the indication of highly *c*-axis oriented AlN thin films that have been grown on the epitaxial 3C-SiC (100) layer.

It is well-known that pre-deposition RF plasma etching can improve the film nucleation and coalescence processes due to removal of impurities. The RF plasma etching can decrease the surface roughness of the 3C-SiC layer and hence can improve the AlN crystal alignment. As shown in Fig. 3, 1- $\mu\text{m}$ -thick AlN films with different RF plasma etching duration of 180 s, 360 s, and 600 s exhibit the full width at half maximum (FWHM) values of  $2.29^\circ$ ,  $1.89^\circ$ , and  $1.73^\circ$ , respectively [14].

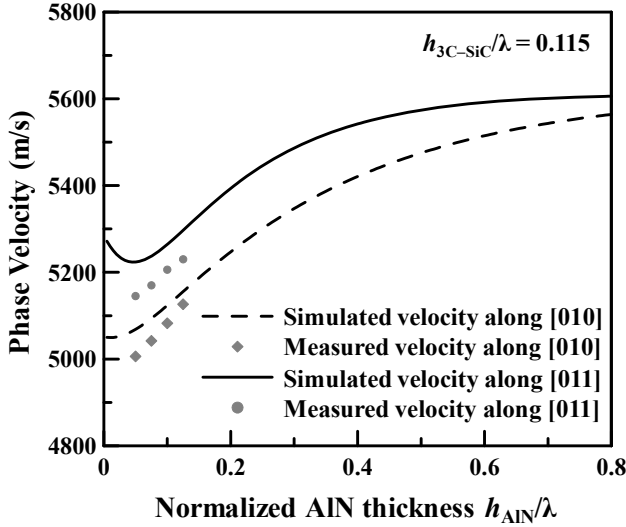


Figure 5. Simulated and measured phase velocities of SAW (Rayleigh mode) propagating along the [010] and [011] directions, respectively.

The cross-sectional scanning electron microscope (SEM, Leo 1550) image of the AlN/3C-SiC/Si composite structure is shown in Fig. 4(a) where the AlN and 3C-SiC film thicknesses are 1  $\mu\text{m}$  and 2.3  $\mu\text{m}$ , respectively. The void defects with trapezoid shape at the 3C-SiC/Si interface are due to silicon outdiffusion. As shown in Fig. 4(b), the AlN seed layer and textured AlN layer can be identified in the bright field (BF) transmission electron microscopy (TEM, Jeol 2100F) image. The AlN thin film exhibits numerous columnar grains, perpendicular to the surface of the epitaxial 3C-SiC layer. The electron diffraction (ED) patterns of 1- $\mu\text{m}$ -thick AlN (0002) thin film along the [110] zone axis are shown in Fig. 4(c). This result supports the conclusion that the AlN grains on the epitaxial 3C-SiC (100) layer are well-textured.

### III. THEORETICAL STUDY OF SAW IN ALN/3C-SiC/Si (100) LAYERED STRUCTURES

In this work, the theoretical analysis of surface acoustic wave characteristics in AlN/3C-SiC/Si composite structures is investigated for the first time. The effective permittivity based on the transfer matrix method was employed to calculate the phase velocity dispersion [3]. The electromechanical coupling coefficients were exactly calculated by the Green's function method. As illustrated in Fig. 1, the crystalline Z-axis of AlN film and the crystalline X-axis of the epitaxial 3C-SiC layer and Si substrate are oriented normal to the surface. The SAW propagation direction is chosen along the crystalline X-axis of the AlN thin film. In the calculation, the AlN film is treated as hexagonal crystal, and the 3C-SiC layer and Si substrate are treated as cubic crystal. The normalized thickness of the epitaxial 3C-SiC is 0.115 and the thickness of the Si substrate is infinite for the theoretical calculation. Their material constants employed in the calculation are obtained from literatures [16]–[18].

In the layered structure, SAW velocity becomes dispersive with respect to the normalized AlN thickness to wavelength [1]–[3]. Fig. 5 shows the phase velocity dispersions of SAW (Rayleigh mode) propagating along the [010] and [011]

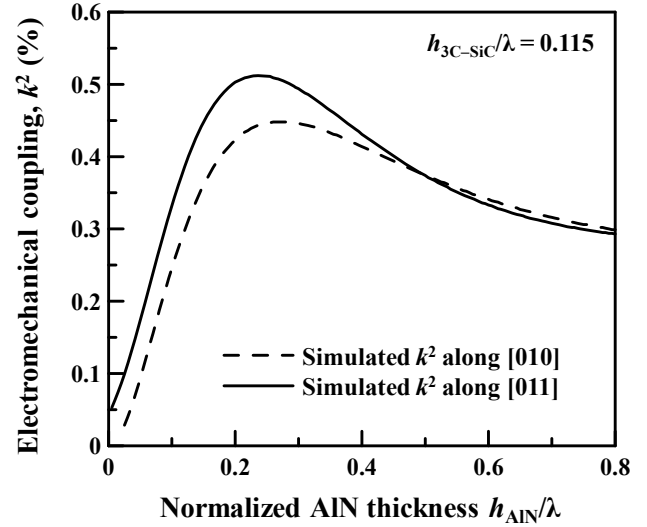


Figure 6. Simulated electromechanical couplings of SAW (Rayleigh mode) propagating along the [010] and [011] directions, respectively.

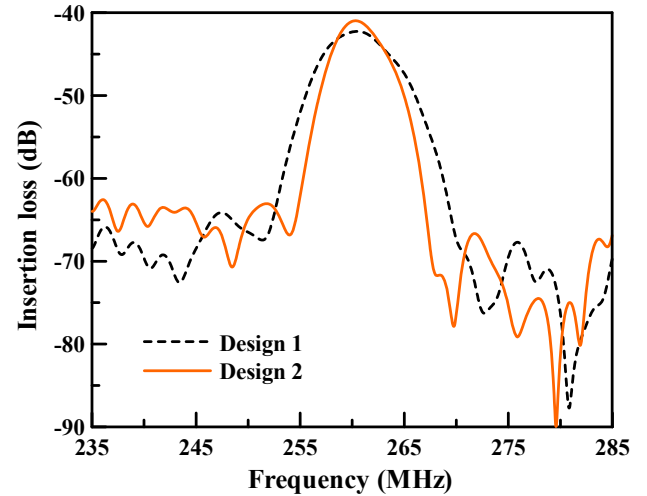


Figure 7. Measured frequency responses of SAW devices on the AlN/3C-SiC/Si layered structure after time-gating for 2- $\mu\text{m}$ -thick AlN thin films and 2.3- $\mu\text{m}$ -thick epitaxial 3C-SiC layers on Si (100) substrates. The SAW propagates along the [011] direction of the 3C-SiC/Si (100) substrate.

directions on AlN/3C-SiC/Si layered structures, respectively. The simulation results show that SAW propagating along the [011] direction has the higher phase velocity than SAW propagating along the [010] direction. As shown in Fig. 6, SAW (Rayleigh mode) propagating along the [011] direction also exhibits the higher electromechanical coupling than SAW propagating along the [010] direction when the normalized AlN thickness ( $h_{\text{AlN}}/\lambda$ ) is smaller than 0.5. The highest electromechanical coupling is approximately 0.51 % when  $h_{\text{AlN}}/\lambda$  is equal to 0.22.

### IV. EXPERIMENTAL RESULTS AND DISCUSSION

In order to generate and detect SAW signals, molybdenum (Mo) interdigital transducers (IDT) with a thickness of 100 nm were fabricated on the surface of the AlN thin films utilizing the lift-off technique. The SAW propagates in the plane normal to the  $c$ -axis of the AlN film and along the [010] and

[011] directions of the 3C–SiC/Si (100) substrate, respectively. The input and output IDTs have 30 and 40 finger pairs with the electrode width of 5  $\mu\text{m}$ . The aperture is 20-wavelength-long (400  $\mu\text{m}$ ) and the delay line is also 400  $\mu\text{m}$ . All dimensions of SAW device are summarized and listed in Table I. The transmission characteristics of the SAW devices were measured using an Agilent E5071B network analyzer.

Figure 7 details the measured frequency response of the SAW device, corresponding to Rayleigh (fundamental) mode, on the AlN/3C–SiC/Si layered structure. The SAW propagates along the [011] direction of the 3C–SiC/Si (100) substrate. The signals were measured using the time-gating method which was employed to remove the feedthrough effect. The Rayleigh mode exhibited a center frequency of 260 MHz as well as a high acoustic velocity up to 5,200 m/s for the 2- $\mu\text{m}$ -thick AlN film and the 2.3- $\mu\text{m}$ -thick epitaxial 3C–SiC film on the Si (100) substrate. As illustrated in Fig. 5, the measured phase velocities are lower than theoretical values because the mass loading of the Mo IDTs was not considered in the calculation. In addition, the measured phase velocities of SAW along the [011] direction are higher than that along the [010] direction by approximately 150 m/s. The measured results consist with the theoretical calculations.

Table I. Dimensions of SAW Devices.

	Design 1	Design 2
IDT pairs	30	40
Aperture	400 $\mu\text{m}$	400 $\mu\text{m}$
Electrode width	5 $\mu\text{m}$	5 $\mu\text{m}$
Delay line	400 $\mu\text{m}$	400 $\mu\text{m}$
Mo electrode thickness	100 nm	100 nm

## V. CONCLUSION

Highly *c*-axis oriented heteroepitaxial AlN thin films were grown on epitaxial 3C–SiC layers on Si (100) substrates using AC reactive magnetron sputtering at temperatures below 450  $^{\circ}\text{C}$ . A two-step deposition process is used to overcome the lattice mismatch of 28.6 % between AlN (0002) and 3C–SiC (100) layers. The lowest FWHM value of 1.31 $^{\circ}$  was achieved with a 3- $\mu\text{m}$ -thick AlN film grown on the epitaxial 3C–SiC (100) layer. In addition, SAW propagation properties in the AlN/3C–SiC/Si composite structure were theoretically analyzed using the effective permittivity and Green's function method. SAW devices with Mo IDTs were fabricated on the AlN/3C–SiC/Si layered structure and the Rayleigh mode propagating along the [011] direction exhibited a high phase velocity up to 5200 m/s. These results confirm that the AlN/3C–SiC/Si composite structure possesses a high acoustic velocity which enables high-frequency layered SAW devices and other types of acoustic devices.

## ACKNOWLEDGMENT

The authors would like to acknowledge the assistance from the Marvell Nanofabrication Laboratory staffs at UC Berkeley.

## REFERENCES

- [1] S. Shikata, H. Nakahata, K. Higaki, A. Hachigo, N. Fujimori, Y. Yamamoto, N. Sakairi, and Y. Takahashi, "1.5GHz SAW bandpass filter using poly-crystalline diamond," in *Proc. IEEE Intl. Ultrason. Symp.*, pp. 277–280, Oct. 1993.
- [2] H. Nakahata, A. Hachigo, K. Higaki, S. Fujii, S. Shikata, and N. Fujimori "Theoretical study on SAW characteristics of layered structures including a diamond layer," *IEEE Trans. Ultrason. Ferroelect. Freq. Control*, vol. 42, pp. 362–375, May 1995.
- [3] T.-T. Wu and Y.-Y. Chen, "Exact analysis of dispersive SAW devices on ZnO/diamond/Si layered structures," *IEEE Trans. Ultrason. Ferroelect. Freq. Control*, vol. 49, pp. 142–149, Jan. 2002.
- [4] M. Werner, S. Klose, F. Szücs, Ch. Moelle, H. J. Fecht, C. Johnston, P. R. Chalker, I. M. Buckley-Golder, "High temperature Young's modulus of polycrystalline diamond," *Diam. Relat. Mater.*, vol. 6, pp. 344–347, Mar. 1997.
- [5] M. Mehregany, C.A. Zorman, S. Roy, A.J. Fleischman, C.-H. Wu, and N. Rajan, "Silicon carbide for micro-electro- mechanical systems," *Int. Mater. Rev.*, vol. 45, pp. 85–108, Mar. 2000.
- [6] I. S. Didenko, F. S. Hickernell, and N. F. Naumenko, "The experimental and theoretical characterization of the SAW propagation properties for zinc oxide films on silicon carbide," *IEEE Trans. Ultrason. Ferroelect. Freq. Control*, vol. 47, pp. 179–187, Jan. 2000.
- [7] J. Y. Kim, H. J. Na, and H. J. Kim, "Surface acoustic wave propagation properties of 3C–SiC epitaxial films on Si(100)," in *Proc. IEEE Intl. Ultrason. Symp.*, pp. 273–276, Oct. 1999.
- [8] V. V. Luchinin, A. V. Korlyakov, and A. A. Vasilev, "Silicon carbide–aluminium nitride: a new high stability composition for MEMS", in *Proc. SPIE*, vol. 3680, pp. 783–791, Mar. 1999.
- [9] R. C. Turner, P. A. Fuierer, R. E. Newnham, and T. R. Shrout, "Materials for high temperature acoustic and vibration sensors: a review", *Appl. Acoustics*, vol. 41, pp. 299–324, 1994.
- [10] T.-T. Yen, C.-M. Lin, X. Zhao, V.V. Felmetzger, D.G. Senesky, M.A. Hopcroft, and A.P. Pisano, "Characterization of aluminum nitride Lamb wave resonators operating at 600 $^{\circ}\text{C}$  for harsh environment RF applications," in *Tech. Dig. IEEE Intl. Conf. Micro Electro Mech. Syst.*, pp. 731–734, Jan. 2010.
- [11] C.-M. Lin, T.-T. Yen, V. V. Felmetzger, M. A. Hopcroft, J. H. Kuypers, and A. P. Pisano, "Thermally compensated aluminum nitride Lamb wave resonators for high temperature applications," *Appl. Phys. Lett.*, vol. 97, 083501, Aug. 2010.
- [12] Y. Takagaki, P. V. Santos, E. Wiebicke, O. Brandt, H.-P. Schonherr, and K. H. Ploog, "Superhigh-frequency surface-acoustic-wave transducers using AlN layers grown on SiC substrates," *Appl. Phys. Lett.*, vol. 81, pp. 2538–2540, Sept. 2002.
- [13] K. Uehara, C.-M. Yang, T. Furusho, S.-K. Kim, S. Kameda, H. Nakase, S. Nishino, and K. Tsubouchi, "AlN epitaxial film on 6H–SiC(0001) using MOCVD for GHz-band SAW devices," in *Proc. IEEE Intl. Ultrason. Symp.*, pp. 905–908, Oct. 2003.
- [14] C.-M. Lin, W.-C. Lien, V. V. Felmetzger, M. A. Hopcroft, D. G. Senesky, and A. P. Pisano, "AlN thin films grown on epitaxial 3C–SiC (100) for piezoelectric resonant devices," *Appl. Phys. Lett.*, vol. 97, 141907, Oct. 2010.
- [15] V. V. Felmetzger, P. N. Laptev, and S. M. Tanner, "Innovative technique for tailoring intrinsic stress in reactively sputtered piezoelectric aluminum nitride films," *J. Vac. Sci. Technol. A*, vol. 27, pp. 417–422, May 2009.
- [16] K. Tsubouchi and N. Mikoshiba, "Zero-temperature-coefficient SAW devices on AlN epitaxial films" *IEEE Trans. Sonics Ultrason.*, vol. 32, pp. 634–644, Sept. 1985.
- [17] B. A. Auld, *Acoustic Fields and Waves in Solids*, Krieger, Florida, 1990.
- [18] K. Karch, P. Pavone, W. Windl, O. Schutt, and D. Strauch, "Ab initio calculation of structural and lattice-dynamical properties of silicon carbide," *Phys. Rev. B*, vol. 50, 17054, Dec. 1994.